

## MASS EXTINCTION

# U-Pb constraints on pulsed eruption of the Deccan Traps across the end-Cretaceous mass extinction

Blair Schoene<sup>1\*</sup>, Michael P. Eddy<sup>1</sup>, Kyle M. Samperton<sup>2</sup>, C. Brenhin Keller<sup>3</sup>, Gerta Keller<sup>1</sup>, Thierry Adatte<sup>4</sup>, Syed F. R. Khadri<sup>5</sup>

Temporal correlation between some continental flood basalt eruptions and mass extinctions has been proposed to indicate causality, with eruptive volatile release driving environmental degradation and extinction. We tested this model for the Deccan Traps flood basalt province, which, along with the Chicxulub bolide impact, is implicated in the Cretaceous-Paleogene (K-Pg) extinction approximately 66 million years ago. We estimated Deccan eruption rates with uranium-lead (U-Pb) zircon geochronology and resolved four high-volume eruptive periods. According to this model, maximum eruption rates occurred before and after the K-Pg extinction, with one such pulse initiating tens of thousands of years prior to both the bolide impact and extinction. These findings support extinction models that incorporate both catastrophic events as drivers of environmental deterioration associated with the K-Pg extinction and its aftermath.

Continental flood basalt provinces are characterized by eruption of >1 million km<sup>3</sup> of basalt over a period of <1 million years (1, 2), representing the largest volcanic events on Earth. Four of the five most severe Phanerozoic mass extinctions [~541 million years (Ma) ago to the present] coincided with emplacement of one of these provinces (3). Although the temporal link between flood basalts and extinctions is well established, the mechanisms by which eruptions drive extinction are poorly understood (4). Two models of environmental change from volcanic activity relate to eruptive volatile emissions (1, 4). The first is volcanogenic CO<sub>2</sub> release, with associated global warming, ocean acidification, and carbon cycle disruption. The second is SO<sub>2</sub> injection into the stratosphere and its conversion to sulfate aerosols, causing global cooling, acid rain, and ecosystem poisoning (5). The predicted time scales of these perturbations contrast sharply. The emission of SO<sub>2</sub> from a single eruption would produce years of cooling, whereas accumulated greenhouse warming from CO<sub>2</sub> can be sustained for many thousands to tens of thousands of years. Testing the effects of this interplay on ecosystems thus requires precisely calibrated volcanic eruption rates that can be correlated to high-resolution climate proxy and biostratigraphic data.

We applied U-Pb zircon geochronology to construct a precise temporal record of eruption

within the Deccan Traps volcanic province, India (Fig. 1). The province is temporally correlated to the K-Pg mass extinction, in which roughly three-fourths of life on Earth was eradicated, including non-avian dinosaurs (6). Previous attempts to constrain eruption rates were limited by poor stratigraphic coverage and/or high analytical uncertainties (7–12). We used U-Pb geochronology by isotope dilution–thermal ionization mass spectrometry (ID-TIMS) (13), which provides analytical uncertainties ( $\pm 2\sigma$ ) as low as 40,000 years (40 ka) for individual dated zircons. Our sampling covers the nine major Deccan formations in the Western Ghats, where the most voluminous (>90% total volume) and complete Deccan exposures are preserved (14–17) (Fig. 1). We sampled both coarse-grained basalts and sedimentary beds between basalt flows that infrequently contain zircon-bearing volcanic ash (11) (fig. S1). These beds, locally termed “redboles,” range from oxidized volcanoclastic material with visible lithic fragments and phenocrysts to paleosol-type horizons produced by in situ weathering of flow tops (18, 19). Of 141 sampled redboles and coarse-grained basalts (Fig. 1 and figs. S1 and S2), 23 redboles and one basalt sample yielded sufficient zircon ( $\geq 5$  crystals) to estimate an eruption age, including four distinct bole horizons and one basalt previously presented by Schoene *et al.* (11). Pristine volcanic crystal morphology indicates minimal transportation or reworking of zircon in a sedimentary environment. Consequently, we inferred that this volcanoclastic, zircon-bearing material was incorporated into redboles as air fall tuff, consistent with some redboles containing a high-SiO<sub>2</sub> (nonbasaltic) component (19), and that these zircons provide a robust means for dating Deccan eruptive stratigraphy.

To estimate the eruption date and associated uncertainty for each sample, we developed an approach using Bayesian statistics to account for the probability distribution of zircon dates and their analytical uncertainties (20) (fig. S6). Although we considered alternative data interpretations (13), they do not affect the conclusions of this study. Twenty-one of 24 dated horizons are from five stratigraphic sections along prominent roads in the Western Ghats, providing complete coverage of the upper four Deccan formations (Fig. 1 and figs. S1 and S2). The remaining three samples span the lower five Deccan formations, where redboles are rare and less likely to contain zircon.

When compiled into a composite stratigraphic section (Fig. 1), almost all samples follow anticipated “younging-up” temporal order based on the independently defined regional stratigraphy (14–17) (figs. S2 and S7). The exception is the Katraj Ghat south of Pune city, where two samples from what was mapped as upper Poladpur Formation are ~100 ka younger than samples near the Poladpur-Ambenali contact in other sections. To resolve this discrepancy, we placed the Poladpur-Ambenali contact in the Katraj Ghat section as ~100 m lower than previously mapped. This simple adjustment does not violate geochemical or geological observations in the stratigraphy, as the Poladpur-Ambenali contact is geochemically transitional in published datasets (14). Furthermore, our placement of the contact is consistent with geochemical studies of the nearby Sinhadag Fort section suggesting that the Poladpur Formation is relatively thin just south of Pune (14).

To further refine the composite stratigraphic age model, we used a Bayesian Markov chain Monte Carlo (MCMC) model in which stratigraphic superposition is imposed on U-Pb zircon dates (13, 21) (Fig. 1). The result is a deposition age estimate for each dated horizon, incorporating dates from all beds above and below each sample to produce an internally consistent age model (Fig. 1). The accuracy of refined age estimates depends solely on sample placement in proper stratigraphic order and is independent of samples’ exact stratigraphic heights.

To calculate volumetric eruption rates through the Deccan Traps, we adopted the volume model of Richards *et al.* (22), in which units of the Wai subgroup (i.e., the Poladpur, Ambenali, and Mahabaleshwar Formations) were interpreted as more voluminous than is apparent from their proportionate thickness in the Western Ghats. This assertion carries nontrivial uncertainties, but we believe it is justified given the correlation of these formations to basalt flows on the province’s periphery, including massive flows that traveled ~1000 km to India’s eastern shore (23, 24). Although different volume models produce changes in the magnitude of calculated eruption rates, the timing of peak eruption rates is unaffected by either the volume model or the interpretation approach of the zircon data (13) (figs. S8 and S9). Additional uncertainty relates to the unconstrained mass and

<sup>1</sup>Department of Geosciences, Princeton University, Princeton, NJ, USA. <sup>2</sup>Nuclear and Chemical Sciences Division, Lawrence Livermore National Laboratory, Livermore, CA, USA.

<sup>3</sup>Berkeley Geochronology Center, Berkeley, CA, USA. <sup>4</sup>ISTE, Institut des Sciences de la Terre, Université de Lausanne, GEOPOLIS, Lausanne, Switzerland. <sup>5</sup>Department of Geology, Amravati University, Amravati, India.

\*Corresponding author. Email: bschoene@princeton.edu

age of Deccan basalt that is currently submerged and inaccessible off India's western shore. We consider this uncertainty to be intractable because current volume models cannot account for this mass component of the province. Consequently, all eruption rates are likely minimum estimates, although we also cannot assess whether the offshore component erupted during the same time intervals as that of the Western Ghats.

We converted our age model into a probabilistic estimate of volumetric flux of basaltic lava using outputs from the MCMC algorithm (Fig. 2). Our results showed that the Deccan Traps erupted in four high-volume events, each lasting  $\leq 100$  ka, separated by periods of relative volcanic quiescence. The first event corresponded to the eruption of the lowermost seven formations

from  $\sim 66.3$  to  $66.15$  Ma ago; the second to the Poladpur Formation from  $\sim 66.1$  to  $66.0$  Ma ago; the third to the Ambenali Formation from  $\sim 65.9$  to  $65.8$  Ma ago; and the fourth and final to the uppermost Mahabaleshwar Formation, from  $\sim 65.6$  to  $65.5$  Ma ago.

Our Deccan eruption model (Fig. 2) constrains the volcanic tempo with high resolution, providing a means to correlate eruption records with biostratigraphic and climate proxy data across the K-Pg extinction. Our model places the second pulse of Deccan volcanism (Poladpur Formation,  $66.1$  to  $66.0$  Ma) as slightly predating a published U-Pb zircon date for the K-Pg boundary (KPB), defined as the Ir anomaly and associated fallout from the Chicxulub impact, within the Denver Basin, Colorado (25). For consistency, we applied the Bayesian approach to that dataset (25) to

estimate a date of  $66.016 \pm 0.050$  Ma ago for the KPB [95% credible interval, internal uncertainties only (13)]. Comparison of our data with recently published  $^{40}\text{Ar}/^{39}\text{Ar}$  geochronology from the Deccan Traps and the Chicxulub impact (12, 26) is currently not possible at the necessary level of precision given systematic bias between the two dating methods, primarily related to uncertainty in ages of  $^{40}\text{Ar}/^{39}\text{Ar}$  fluence monitors and the values of the  $^{40}\text{K}$  decay constant and physical constants (13). Assuming that the Chicxulub impact coincides exactly with the main phase of extinction, the MCMC model outputs from our Deccan data demonstrate a  $\sim 90\%$  probability that the Poladpur Formation eruption pulse began tens of thousands of years before the K-Pg mass extinction event.

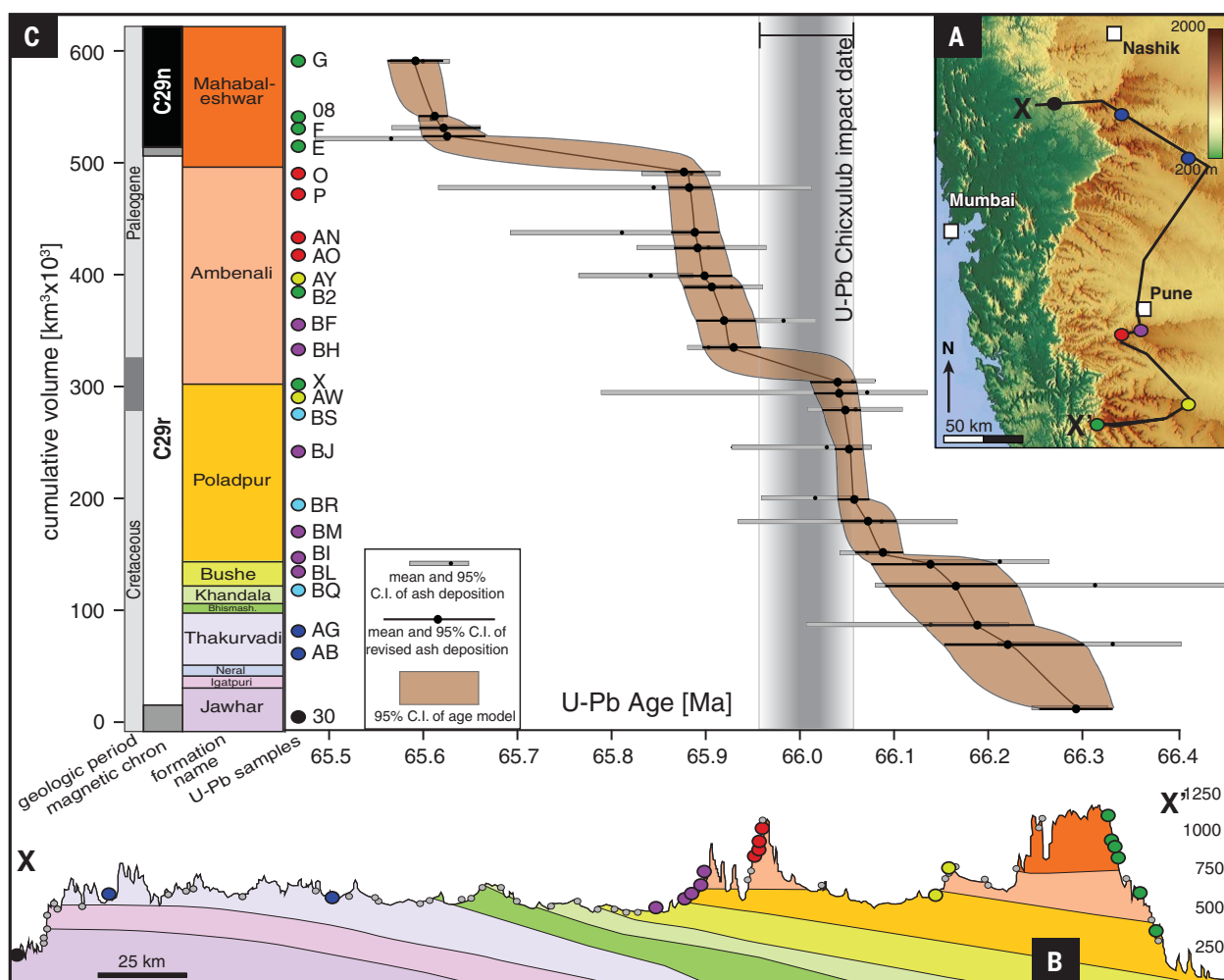
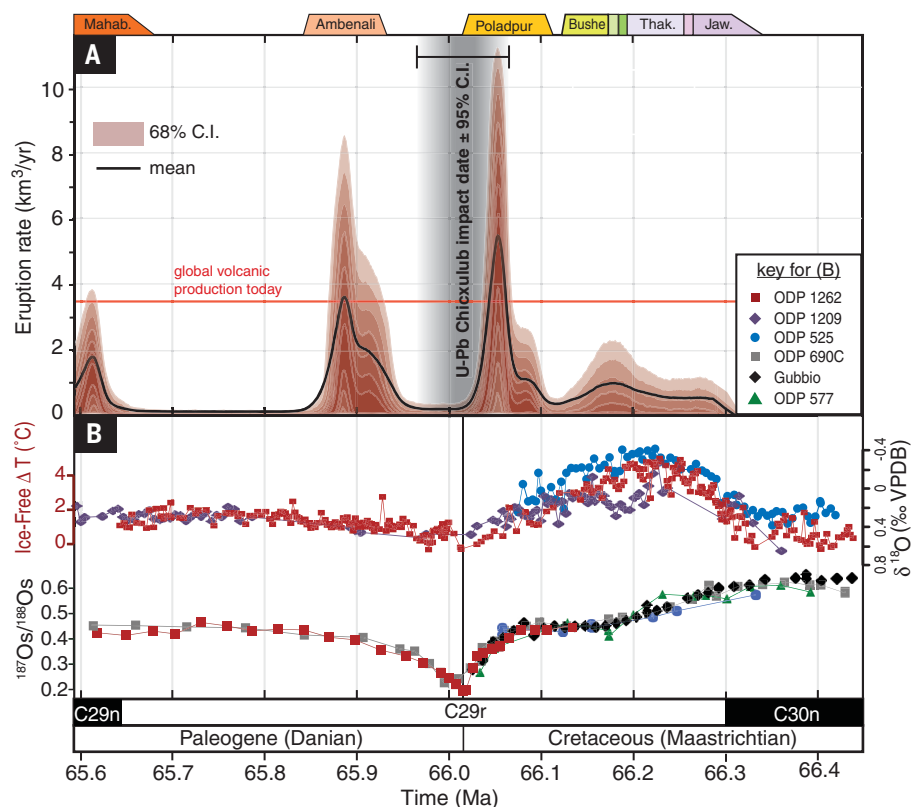


**Fig. 1. Stratigraphy, sampling transects, and U-Pb age model for the Deccan Traps.** (A) Elevation map of study location in the Western Ghats, India. A black segmented line denotes cross section X-X' as shown in (B). Sampling transects are located by colored dots. (B) Geologic cross section through the field area, with sample locations indicated. Different basalt formations in the Deccan Traps are color-coded to the stratigraphic column in (C). Cross section is based on previous work (14–17), modified according to our geochronology. (C) Volumetric stratigraphic column and magnetic

chrons of the major formations of the Deccan Traps (22, 45). The plotted sample heights ("RB" sample prefix omitted) are based on the composite stratigraphic section compiled in fig. S2. The age model for the Deccan Traps, based on our U-Pb geochronology, is shown with 95% credible intervals. Horizontal gray bars indicate eruption ages derived from populations of zircon dates from each horizon; black horizontal bars show dates refined from the stratigraphic Bayesian model. The vertical gray-shaded bar shows an age for the Chicxulub impact (25).

## Fig. 2. Eruption rate model for the Deccan Traps, based on U-Pb geochronology.

(A) Results from the MCMC algorithm used to generate the age model in Fig. 1, converted to a probabilistic volumetric eruption rate for the Deccan Traps shown with contours up to 68% credible intervals. The U-Pb date for the Chicxulub impact is the same as in Fig. 1. Total global volcanic productivity ( $\sim 3$  to  $4 \text{ km}^3/\text{year}$ ) includes mid-ocean ridges and volcanic arcs (28). (B) Compilation of proxy records from ODP cores and outcrops. Upper data points are  $\delta^{18}\text{O}$  of species-specific benthic foraminifera from ODP 525 (46), ODP 1262 (36), and ODP 1209 (37); VPDB, Vienna PeeDee Belemnite standard. Temperature is calculated for benthic foraminifera *Nuttallides truempyi* in ODP 1262 (36). Osmium isotopic records come from bulk carbonate from both ODP cores and outcrop (40, 41). Age models are described in (13).



The K-Pg extinction preserves the only known mass extinction that coincides with both a large igneous province and a bolide impact. As such, several hypotheses have been forwarded in which the impact triggered or modulated volcanic eruptions. Although the most recent iteration of this hypothesis concedes initiation of Deccan eruptions several hundred thousand years before the impact, it proposes that impact-induced seismicity increased eruption rates in the Deccan Traps and at mid-ocean ridges through evacuation of preexisting magma chambers in the upper mantle and lower crust (12, 22, 27). It is unlikely that our Deccan eruptive history is consistent with this model, given the high probability that the Poladpur pulse began before the impact by tens of thousands of years, followed by an eruption hiatus of  $\leq 100$  ka after the impact.

Estimates for the entire volcanic flux on Earth today are 3 to  $4 \text{ km}^3/\text{year}$  (28), indicating on average a doubling in global volcanic activity for  $\leq 100$  ka during each of the four high-volume Deccan eruptive events, but requiring periods of  $> 5$  to 10 times the global average. In fact, groups of flows within the Poladpur and Mahabaleshwar Formations, each potentially comprising  $> 50,000 \text{ km}^3$ , lack secular evolution in paleomagnetic poles, suggesting eruption over decades to centuries (29). Such high eruption rates of  $> 1000 \text{ km}^3/\text{year}$  are permitted by our U-Pb geochronology, requiring hiatuses of hundreds to thousands of years within our resolved pulses so as not to exceed total volume estimates. In addition to being con-

sistent with brief but extreme eruption rates, our data demonstrate that the Deccan Traps erupted in pulses with durations of  $\sim 100$  ka, providing insight into tempos of melt production and/or transport in the upper mantle and lower crust (30, 31).

Our eruption rate model is a first step toward robustly evaluating the environmental impacts associated with Deccan volcanism. The most commonly cited contributors to environmental change associated with flood basalts are  $\text{CO}_2$  (warming),  $\text{SO}_2$  (cooling upon conversion to sulfate aerosols), and chemical weathering of fresh basaltic material (cooling via  $\text{CO}_2$  drawdown). For single continental flood basalt flows that erupt over a few decades, volcanic  $\text{SO}_2$  has been modeled to drive cooling of  $5^\circ$  to  $10^\circ\text{C}$  for the duration of the eruption (5), after which acid rain rapidly removes sulfur compounds from the atmosphere. For persistent cooling over many thousands of years, therefore, hiatuses of only several decades between eruptions are required (5).

In contrast to  $\text{SO}_2$ , the time scale of  $\text{CO}_2$  removal from the ocean-atmosphere system is slow:  $\sim 1$  ka,  $\sim 10$  ka, and  $\sim 100$  ka for mixing into the deep ocean, reaction with sediments, and removal by silicate weathering, respectively (32, 33). As a result, although climate effects during an eruptive event may be dominated by cooling associated with elevated sulfate aerosols, accumulation of volcanic  $\text{CO}_2$  emissions can lead to net warming on intermediate time scales between eruptive events. On time scales of hundreds of ka to  $> 1$  Ma, weathering of fresh basalt has been modeled to

result in net  $\text{CO}_2$  drawdown and cooling, especially if the basalt is at low latitudes, as were the Deccan Traps (34).

As an initial attempt to correlate our eruptive history with paleoenvironmental data, we used two proxy records across the K-Pg transition (Fig. 2B). Benthic foraminifera  $\delta^{18}\text{O}$  compositions indicate  $\sim 2^\circ$  to  $4^\circ\text{C}$  of deep ocean warming over  $\sim 150$  ka, beginning at the C30n-C29r magnetic reversal ( $\sim 66.3$  Ma ago), followed by cooling over  $\sim 150$  ka prior to the KPB (35–37). It has also been argued on the basis of  $\delta^{18}\text{O}$  data from Elles, Tunisia, that renewed warming began tens of thousands of years before the KPB (38) (fig. S11).

Initial warming at  $\sim 66.3$  Ma ago and a coeval increase in carbonate dissolution have been interpreted as resulting from volcanogenic  $\text{CO}_2$  buildup and consequent ocean acidification (35), which our geochronology shows to have occurred during the initial pulse of Deccan eruptions. Warming curtailed toward the end of the first pulse, and cooling began before and continued through the initiation of the Poladpur Formation eruptions (Fig. 2). The extrusion of the voluminous Poladpur Formation may have resulted in short periods of  $\text{SO}_2$ -driven cooling that could have continued to promote the overall cooling trend, but cooling for tens of thousands of years due to  $\text{SO}_2$  emissions is difficult to sustain given the predicted short residence time of sulfate aerosol (1, 5). Alternatively, an increase in surface area of exposed basalt associated with the Poladpur eruptions is possible given current Deccan stratigraphic area/volume models (22),



resulting in enhanced basalt weathering, CO<sub>2</sub> drawdown, and continued global cooling during the tens of thousands of years before the extinction. If periods of cooling did result from sulfate aerosols during the Poladpur eruptions, the short intervals of temperature decrease could have slowed silicate weathering and associated CO<sub>2</sub> drawdown, thus permitting CO<sub>2</sub> buildup in the atmosphere that would be manifest between punctuated eruptions within the Poladpur Formation (39).

Testing whether basalt weathering was important leading up to the KPB is aided through study of the Os isotope system in marine carbonates because the ocean residence time of Os is short and basaltic <sup>187</sup>Os/<sup>188</sup>Os is low [0.1 (10)] relative to late Mesozoic seawater [0.6 (40)]. Published Os isotopic data from marine carbonates (40) show a marked decrease toward mantle values beginning at the onset of Deccan volcanism (Fig. 2B). A second downturn in <sup>187</sup>Os/<sup>188</sup>Os, beginning tens of thousands of years before the KPB, has been interpreted as a downward redistribution of extraterrestrial Os derived from the Chicxulub impactor (40, 41). However, this decrease is synchronous with the Poladpur eruption pulse and is thus also consistent with increased weathering of a more extensive Deccan basalt pile.

Post-extinction and post-Chicxulub benthic foraminifera δ<sup>18</sup>O and carbonate Os isotopic records do not covary with the Deccan eruption record. However, the Os record does not recover to the pre-Deccan <sup>187</sup>Os/<sup>188</sup>Os value either, perhaps indicating that a steady state was reached between basalt production and weathering despite continued eruptions. Regardless, the starkly different responses of O and Os isotope records during the post-extinction recovery require models that explicitly incorporate the effects of continued Deccan eruptions, the Chicxulub impact, and biotic effects on the carbon cycle in a world with devastated ecosystems.

Although the initiation of a massive eruptive pulse shortly before the Chicxulub impact and mass extinction supports a Deccan contribution to ecosystem collapse, much remains to be discovered as to how flood basalt magmatism contributes to mass extinctions. U-Pb geochronology has shown that, similar to the K-Pg extinction, the end-Permian (~252 Ma ago) and end-Triassic (~201 Ma ago) mass extinctions occurred on short time scales (< tens of ka), hundreds of thousands of years after the onsets of the Siberian Traps and Central Atlantic Magmatic Province flood basalt

provinces, respectively (42–44). The eruptions and associated intrusive magmatism are presumed to have driven rapid extinction despite this time lag and the absence of bolide impacts. This lag between the onset of magmatism and extinction may be a result of highly nonlinear rates of magmatism, as documented here for the Deccan Traps. Continuing to study other flood basalt provinces will clarify the importance of eruptive and intrusive tempo in driving ecosystem collapse and extinction. Such an understanding of biosphere sensitivity and the importance of threshold processes during climate change is as relevant today as for these catastrophic events in Earth history.

## REFERENCES AND NOTES

1. S. Self, A. Schmidt, T. A. Mather, *Geol. Soc. Am. Spec. Pap.* **505**, 319–337 (2014).
2. S. E. Bryan et al., *Earth Sci. Rev.* **102**, 207–229 (2010).
3. V. E. Courtillot, P. R. Renne, C. R. Geosci. **335**, 113–140 (2003).
4. D. P. G. Bond, P. B. Wignall, *Geol. Soc. Am. Spec. Pap.* **505**, 29–55 (2014).
5. A. Schmidt et al., *Nat. Geosci.* **9**, 77–82 (2016).
6. J. J. Sepkoski, in *Global Events and Event Stratigraphy in the Phanerozoic*, O. H. Walliser, Ed. (Springer, 1996), pp. 35–51.
7. R. A. Duncan, D. G. Pyle, *Nature* **333**, 841–843 (1988).
8. V. Courtillot et al., *Nature* **333**, 843–846 (1988).
9. A. Chenet, X. Quidelleur, F. Fluteau, V. Courtillot, S. Bajpai, *Earth Planet. Sci. Lett.* **263**, 1–15 (2007).
10. C. Allegre, J. Birck, F. Capmas, V. Courtillot, *Earth Planet. Sci. Lett.* **170**, 197–204 (1999).
11. B. Schoene et al., *Science* **347**, 182–184 (2015).
12. P. R. Renne et al., *Science* **350**, 76–78 (2015).
13. See supplementary materials.
14. J. E. Beane, C. A. Turner, P. R. Hooper, K. V. Subbarao, J. N. Walsh, *Bull. Volcanol.* **48**, 61–83 (1986).
15. A. E. Jay, M. Widdowson, *J. Geol. Soc. London* **165**, 177–188 (2008).
16. S. Khadri, K. Subbarao, P. Hooper, J. Walsh, *Geol. Soc. India Mem.* **10**, 281 (1988).
17. C. W. Devey, P. C. Lightfoot, *Bull. Volcanol.* **48**, 195–207 (1986).
18. M. Widdowson, J. N. Walsh, K. V. Subbarao, *Geol. Soc. London Spec. Publ.* **120**, 269–281 (1997).
19. P. Ghosh, M. R. G. Sayeed, R. Islam, S. M. Hudekari, *Palaeogeogr. Palaeoclimatol. Palaeoecol.* **242**, 90–109 (2006).
20. C. B. Keller, B. Schoene, K. M. Samperton, *Geochem. Perspect. Lett.* **8**, 31–35 (2018).
21. C. E. Buck, C. D. Litton, A. F. Smith, *J. Archaeol. Sci.* **19**, 497–512 (1992).
22. M. A. Richards et al., *GSA Bull.* **127**, 1507–1520 (2015).
23. K. B. Knight, P. R. Renne, A. Halkett, N. White, *Earth Planet. Sci. Lett.* **208**, 85–99 (2003).
24. S. Self, A. E. Jay, M. Widdowson, L. P. Keszthelyi, *J. Volcanol. Geotherm. Res.* **172**, 3–19 (2008).
25. W. C. Clyde, J. Ramezani, K. R. Johnson, S. A. Bowring, M. M. Jones, *Earth Planet. Sci. Lett.* **452**, 272–280 (2016).
26. P. R. Renne et al., *Science* **339**, 684–687 (2013).
27. J. S. Byrnes, L. Karlstrom, *Sci. Adv.* **4**, eaao2994 (2018).
28. J. A. Crisp, *J. Volcanol. Geotherm. Res.* **20**, 177–211 (1984).
29. A.-L. Chenet, F. Fluteau, V. Courtillot, M. Gérard, K. V. Subbarao, *J. Geophys. Res.* **113**, B04101 (2008).
30. L. Karlstrom, M. Richards, *J. Geophys. Res. Solid Earth* **116**, B08216 (2011).
31. B. A. Black, M. Manga, *Earth Planet. Sci. Lett.* **458**, 130–140 (2017).
32. D. Archer, E. Maier-Reimer, *Nature* **367**, 260–263 (1994).
33. C. Dessert, B. Dupré, J. Gaillardet, L. M. François, C. J. Allegre, *Chem. Geol.* **202**, 257–273 (2003).
34. C. Dessert et al., *Earth Planet. Sci. Lett.* **188**, 459–474 (2001).
35. M. J. Henehan, P. M. Hull, D. E. Penman, J. W. Rae, D. N. Schmidt, *Philos. Trans. R. Soc. London Ser. B* **371**, 20150510 (2016).
36. J. S. Barnett et al., *Geology* **46**, 147–150 (2017).
37. T. Westerhold, U. Röhl, B. Donner, H. K. McCarren, J. C. Zachos, *Palaeogeogr. Palaeoclimatol. Palaeoecol.* **441**, 152–164 (2016).
39. M. Mussard, G. Le Hir, F. Fluteau, V. Lefebvre, Y. Goddérès, *Geol. Soc. Am. Spec. Pap.* **505**, 1–14 (2014).
40. N. Robinson, G. Ravizza, R. Coccioni, B. Peucker-Ehrenbrink, R. Norris, *Earth Planet. Sci. Lett.* **281**, 159–168 (2009).
41. G. Ravizza, D. Vonderhaar, *Palaeogeogr. Palaeoclimatol. Palaeoecol.* **27**, PA3219 (2012).
42. J. H. F. L. Davies et al., *Nat. Commun.* **8**, 15596 (2017).
43. S. D. Burgess, S. A. Bowring, *Sci. Adv.* **1**, e1500470 (2015).
44. B. Schoene, J. Guex, A. Bartolini, U. Schaltegger, T. J. Blackburn, *Geology* **38**, 387–390 (2010).

## ACKNOWLEDGMENTS

This paper benefited from comments made by three anonymous reviewers and discussions with A. Maloof and J. Higgins. Field assistance was provided by M. Coronado, P. Kemeny, and V. Sordet. J. Puneekar provided critical field assistance and sample recollection. We also thank A. Chen, S. Gwizd, A. Hager, and D. Okhai for tirelessly separating zircons from redbole samples. **Funding:** Field and lab work was supported by NSF grant EAR-1454430 (B.S. and G.K.) and by the Princeton Department of Geosciences Scott Fund. Lawrence Livermore National Laboratory is operated by Lawrence Livermore National Security LLC for the U.S. Department of Energy, National Nuclear Security Administration under contract DE-AC52-07NA27344. This paper is LLNL contribution LLNL-JRNL-755419. **Author contributions:** All authors except C.B.K. participated in fieldwork and sample collection; U-Pb geochronology was done by K.M.S., M.P.E., and B.S.; Bayesian modeling was done by C.B.K., K.M.S., and B.S.; and the manuscript and figures were prepared by B.S., M.P.E., and K.M.S. with input from G.K., T.A., C.B.K., and S.F.R.K. **Competing interests:** The authors have no competing interests to declare. **Data and materials availability:** All methods, data, and codes used for modeling are available in the manuscript or supplementary materials.

## SUPPLEMENTARY MATERIALS

www.sciencemag.org/content/363/6429/862/suppl/DC1  
Materials and Methods  
Supplementary Text  
Figs. S1 to S11  
Tables S1 to S3  
References (45–106)

27 July 2018; accepted 8 January 2019  
10.1126/science.aau2422

## U-Pb constraints on pulsed eruption of the Deccan Traps across the end-Cretaceous mass extinction

Blair Schoene, Michael P. Eddy, Kyle M. Samperton, C. Brenhin Keller, Gerta Keller, Thierry Adatte and Syed F. R. Khadri

*Science* **363** (6429), 862-866.  
DOI: 10.1126/science.aau2422

### Two timelines for extinction

The Cretaceous-Paleogene extinction that wiped out the nonavian dinosaurs 66 million years ago was correlated with two extreme events: The Chicxulub impact occurred at roughly the same time that massive amounts of lava were erupting from the Deccan Traps (see the Perspective by Burgess). Sprain *et al.* used argon-argon dating of the volcanic ash from the Deccan Traps to argue that a steady eruption of the flood basalts mostly occurred after the Chicxulub impact. Schoene *et al.* used uranium-lead dating of zircons from ash beds and concluded that four large magmatic pulses occurred during the flood basalt eruption, the first of which preceded the Chicxulub impact. Whatever the correct ordering of events, better constraints on the timing and rates of the eruption will help elucidate how volcanic gas influenced climate.

*Science*, this issue p. 866, p. 862; see also p. 815

#### ARTICLE TOOLS

<http://science.sciencemag.org/content/363/6429/862>

#### SUPPLEMENTARY MATERIALS

<http://science.sciencemag.org/content/suppl/2019/02/20/363.6429.862.DC1>

#### RELATED CONTENT

<http://science.sciencemag.org/content/sci/363/6429/815.full>  
<http://science.sciencemag.org/content/sci/363/6429/866.full>

#### REFERENCES

This article cites 105 articles, 25 of which you can access for free  
<http://science.sciencemag.org/content/363/6429/862#BIBL>

#### PERMISSIONS

<http://www.sciencemag.org/help/reprints-and-permissions>

Use of this article is subject to the [Terms of Service](#)